Original Article

On Frequencies of Non-Uniform Rhombic Plate to Mitigate Unwanted Vibration

Narinder Kaur [1, ✉], Samta Jain [1], Anupam Khanna [2]

1. *Department of Mathematics, Statistics and Physics, Punjab Agricultural University, Ludhiana, IND*
2. *Department of Mathematics, Kurukshetra University, Kurukshetra, IND*

Received: March 18, 2026 | Review began: April 17, 2026 | Review ended: May 19, 2026 | Published: June 30, 2026

Abstract

This study presents a comprehensive analysis of the vibration behavior of a rhombic tapered plate exposed to a two-dimensional temperature distribution. The plate's thickness is modeled with a bilinear variation, while material non-homogeneity is introduced through an exponential variation of density along the x-direction. Employing the Rayleigh-Ritz method, the governing differential equation is formulated using classical plate theory and solved to obtain the natural frequencies corresponding to the first two modes of vibration. A detailed parametric study is conducted by varying key structural and thermal parameters, including the non-homogeneity index, thermal gradient, aspect ratio, and taper constant. The analysis is carried out for two distinct boundary conditions: fully clamped (C-C-C-C) and fully simply supported (SS-SS-SS-SS). However, the present analysis is limited to linear viscoelastic behavior, small deflection assumptions, and idealized boundary conditions. The results, presented in tabular form, highlight the significant influence of both thermal and geometric factors on the vibrational response of the structure. The study offers valuable insights into the influence of the thermal gradient and structural parameters on the vibration behavior of plate structures.

Categories: Structural Engineering

Keywords: tapered, non-homogeneity, structural parameter, rhombic, vibration

Introduction

The dynamic analysis of plate-type structures has become an important topic of research because such structural elements are extensively used in aircraft panels, ship structures, bridges, mechanical devices, and thermal engineering components. In practical applications, these structures often operate under non-uniform temperature environments, due to which the elastic properties and stiffness of the material undergo significant changes. Moreover, the presence of variable thickness, material non-homogeneity, and skew geometry considerably alters the vibrational response of the structure. Among various geometrical configurations, rhombic plates possess special importance owing to their structural efficiency and suitability in complex engineering designs. The frequency of such plates under different conditions needs thorough investigation to ensure their effectiveness and safety.

Chakraverty [1] provided a detailed study about the vibrational behavior of two-dimensional plates. Chakraverty and Pradhan [2] carried out a dynamic analysis of functionally graded rectangular plates under various boundary conditions. Gorman [3] figured out the complete and accurate solution for the free vibrations of rhombic plates. Leissa et al. [4] analyzed the free vibration of rectangular plates with non-uniform elastic edge constraints using exact solutions and the Ritz method, presenting numerical results for rotational restraints with parabolic variation.

Azam et al. [5] investigated rhombic plates with a central crack using Finite Element Method, showing that the natural frequency decreases with increasing crack length and skew angle, with minimal reduction at low crack ratios. The impact of thermal conditions on the vibrations of a linearly tapered parallelogram plate [5] and bi-linearly tapered parallelogram plate [6] was investigated. Ansari et al. [7] analyzed functionally graded material rhombic plates and showed that the frequency decreases with increasing volume fraction index and cutout size, increases with skew angle, and is largely unaffected by additional mass. Free vibrations of a simply supported plate with stress singularities at two obtuse corners are reported [8]. Kaur et al. [9] discussed the vibration of tapered triangular plates with different boundary conditions. Khanna and Kaur [10] examined the vibration of a rectangular plate with parabolic thickness variation and a bi-directional temperature distribution. The impact of one-dimensional thermal effect with variable thickness on the vibration of a square plate is illustrated [11].

Khanna et al. [12] examined the effect of non-homogeneity on the vibration of a clamped square plate. The initial two frequency modes of a visco-elastic square plate are obtained under thermal influence [13]. Leissa [14] provided valuable data on the vibration of plates of various shapes with different boundary conditions in the form of a monograph. Li [15] worked on vibrations of a rectangular plate with general elastic boundary supports. Malhotra et al. [16] studied the effect of fiber alignment on the natural frequencies of thin, rhombic orthotropic plates. Singha et al. [17] applied a shear deformable finite element to analyze the vibration properties of thermally stressed laminated composite skew plates. A differential quadrature approach was used to perform numerical analysis on the free vibration of rhombic plates with unrestricted edges [18].

A considerable amount of research has been carried out on the vibration analysis of plate structures under different geometrical, thermal, and material conditions. Several researchers have investigated the effect of tapering, thermal loading, skew geometry, and material non-homogeneity individually or in limited combinations. However, very limited attention has been devoted to the vibration behavior of non-homogeneous bilinearly tapered rhombic plates subjected simultaneously to a two-dimensional thermal distribution and varying thermal gradients. The combined influence of tapering parameters, skew geometry, thermal effects, and material non-homogeneity on the vibration characteristics of rhombic plates has not been discussed comprehensively in the existing literature. Therefore, the present study attempts to fill this research gap by developing a unified analytical model for such complex structural configurations. Frequencies for the first two modes of vibration at various values of structural parameters are calculated for two boundary conditions, i.e., C-C-C-C and SS-SS-SS-SS. After analyzing the impact of thermal gradient and other structural parameters on vibration modes and frequencies, the study seeks to provide valuable insights for the design and optimization of such plates to control unwanted vibrations.

Materials And Methods

Geometry of the plate

In the present study, a non-homogeneous tapered thin rhombic plate is considered with two boundary conditions i.e. fully clamped and fully simply supported. Figure *1* represents the discussed tapered rhombic plate OABC with sides "a" and skew angle "θ" in Cartesian co-ordinates X and Y. A skew coordinate system (x,y) is introduced along the edges of the rhombus to simplify the mathematical foundation.

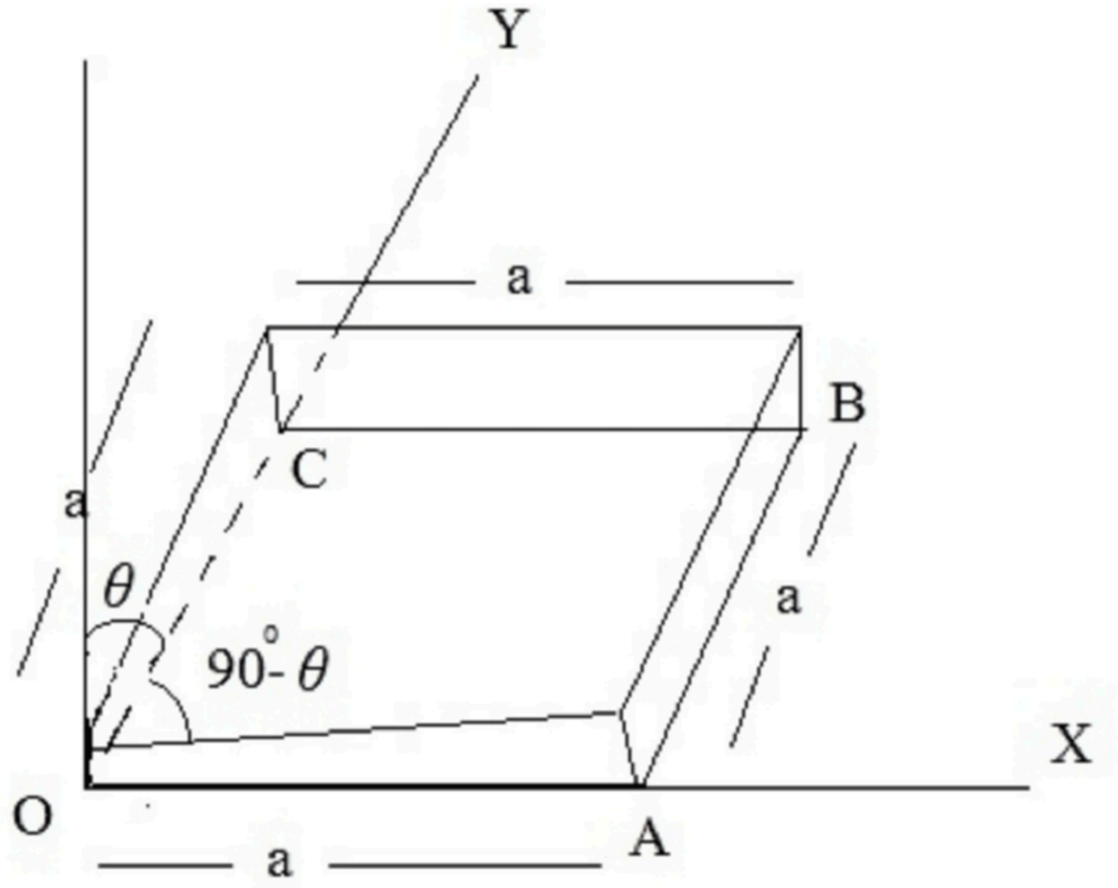

FIGURE 1: Bilinear tapered rhombic plate with sides "a" and skew angle "θ"

Frequency equation

The Rayleigh-Ritz method used to derive the frequency equation relies on the principle of energy conservation, ensuring that the maximum strain energy (V) must be equal to the maximum kinetic energy (T). Therefore, it is necessary for the problem under consideration [10]:

$$\delta(V - T) = 0 \tag{1}$$

where V and T are defined as follows [11]:

where

$$T = \frac{1}{2}\rho\omega^2 \int_0^a \int_0^a hW^2 \, dX \, dY \tag{2}$$

and

$$V = \frac{1}{2}\int_0^a \int_0^a D_1 \left[W_{XX}^2 + W_{YY}^2 + 2\nu W_{XX}W_{YY} + 2(1-\nu)W_{XY}^2\right] dX \, dY \tag{3}$$

Here, D_1 is the flexural rigidity of the rhombic plate as [12]:

$$D_1 = \frac{Eh^3}{12(1-\nu^2)} \tag{4}$$

In order to make calculations simple and fast, the coordinates X and Y are converted into skew coordinates x and y as follows [1]:

$$\begin{aligned} X &= x + y\sin\theta, \\ Y &= y\cos\theta, \\ dX &= dx, \quad dY = \cos\theta\, dy \end{aligned} \tag{5}$$

Substitute equation (5) in equation (2) and equation (6) one gets:

$$T_1 = \frac{1}{2}\rho\omega^2 \int_0^a \int_0^a (\cos\theta) h W^2\, dx\, dy \tag{6}$$

$$\begin{aligned} V_1 = \frac{1}{2\cos^3\theta} \int_0^a \int_0^a \Big[& D_1 (W_{xx})^2 - 4\sin\theta\, W_{xx} W_{xy} + 2(\sin^2\theta + \nu\cos^2\theta) W_{xx} W_{yy} \\ & + 2(1 + \sin^2\theta - \nu\cos^2\theta)(W_{xy})^2 - 4\sin\theta\, W_{xy} W_{yy} + (W_{yy})^2 \Big]\, dx\, dy \end{aligned} \tag{7}$$

Model assumptions

Temperature Variation in the Plate

Since a majority of machines or mechanical systems operate in conditions with significant temperature fluctuations, it is necessary to analyze the impact of temperature on the vibrational characteristics of the structure. In the present study, the authors assumed a bilinear thermal variation as [1]:

$$\tau = \tau_0 \left(1 - \frac{x}{a}\right)\left(1 - \frac{y}{a}\right)$$

The variation in the modulus of elasticity with temperature for the majority of engineering materials can be described [6]:

$$E = E_0(1 - \gamma\tau)$$

Here, E_0 is the Young's modulus at a reference temperature τ_0 and γ signifies slope of the variation of E with τ. After replacing value of τ in E it transforms into:

$$E = E_0 \left(1 - \alpha\left(1 - \frac{x}{a}\right)\left(1 - \frac{y}{b}\right)\right) \tag{8}$$

where $\alpha = \gamma\tau_0$ ($0 \le \alpha < 1$) is thermal gradient.

Thickness Variation

As plates with variable thicknesses are widely used in mechanical structures and designs, it is essential to assess the impact of non-uniform thickness variations on the vibration of the structure or design. Hence, the authors studied a bi-linear variation in thickness as follows [6]:

$$h = h_0 \left(1 + \beta_1 \frac{x}{a}\right)\left(1 + \beta_2 \frac{y}{a}\right) \tag{9}$$

where β_1 and β_2 are the taper constants and h_0 is the thickness of the plate at x=y=0.

Non-Homogeneity in the Plate's Material

Presence of non-homogeneity directly affects the material density of the plate. In this work, the density variation in the x-direction is assumed to be exponential as [1]:

$$\rho = \rho_0 e^{\frac{\alpha_1 x}{a}} \tag{10}$$

where, ρ_0 is density at x=0 and α_1 is non-homogeneity constant.

After using equations (8), and (9) in equation (4), one gets:

$$D_1 = \frac{E_0\left(1-\alpha\left(1-\frac{x}{a}\right)\left(1-\frac{y}{a}\right)\right)h_0^3\left(1+\beta_1\frac{x}{a}\right)^3\left(1+\beta_2\frac{y}{a}\right)^3}{12(1-\nu^2)} \tag{11}$$

Boundary Condition

In this paper, two distinct boundary conditions i.e. fully clamped boundary (C-C-C-C) and fully simply supported boundary (SS-SS-SS-SS) are discussed as follows:

For a fully clamped rhombic plate, the boundary conditions are shown as [7]:

$$\begin{aligned} W=0, \quad W_x=0 \quad \text{at} \quad x=0 \,\&\, x=a \\ W=0, \quad W_y=0 \quad \text{at} \quad y=0 \,\&\, y=a \end{aligned} \tag{12}$$

A set of algebraic and partial differential equations for the simply supported boundary condition is presented as [7]:

$$W=0,\ M_x=0 \quad \text{at } x=0 \,\&\, x=a, \qquad W=0,\ M_y=0 \quad \text{at } y=0 \,\&\, y=a \tag{13}$$

To satisfy the above two boundary conditions and to ensure continuity and differentiability over the domain, the associated deflection function is taken as to satisfy the above two boundary conditions, the associated deflection function is taken as [1]:

$$W = R^m\,[A_1 + A_2R], \qquad m=1,2 \tag{14}$$

where

$$R = \left(\frac{x}{a}\right)\left(\frac{y}{a}\right)\left(1-\frac{x}{a}\right)\left(1-\frac{y}{a}\right)$$

and A_1 and A_2 are arbitrary constants. Such polynomial-based admissible functions are commonly used due to their computational efficiency and convergence properties. Here m = 1 for simply supported boundary and m = 2 for fully clamped boundary.

Solution of frequency equation

To simplify and standardize the problem, non-dimensionalization is applied as:

$$\varphi = \frac{x}{a}, \qquad \eta = \frac{y}{a} \tag{15}$$

Substitute equation (15) in equations (6) and (7), one obtains

$$T_2 = \frac{1}{2}h_0\rho_0\omega^2a^2\int_0^1\int_0^1(1+\beta_1\varphi)(1+\beta_2\eta)e^{\alpha_1\varphi}W^2\cos\theta\,d\varphi\,d\eta \tag{16}$$

and

$$\begin{aligned} V_2 = \frac{E_0h_0^3}{24a^2(1-\nu^2)}\int_0^1\int_0^1 &\frac{(1-\alpha(1-\varphi)(1-\eta))(1+\beta_1\varphi)^3(1+\beta_2\eta)^3}{\cos^3\theta} \\ &\times\Big[W_{\varphi\varphi}^2 - 4\sin\theta\,W_{\varphi\varphi}W_{\eta\eta} + W_{\eta\eta}^2 + 2(1+\sin^2\theta-\nu\cos^2\theta)\,W_{\varphi\varphi}W_{\eta\eta} \\ &+2(1+\nu\cos^2\theta)\,W_{\varphi\eta}^2 - 4\sin\theta\,W_{\eta\eta}W_{\varphi\eta}\Big]\,d\varphi\,d\eta \end{aligned} \tag{17}$$

On using equation (16) and equation (17) in equation (1), we obtain:

$$\delta\left(V_3 - \lambda^2 T_3\right) = 0 \tag{18}$$

where

$$T_3 = \int_0^1 \int_0^1 (1+\beta_1\phi)(1+\beta_2\eta)e^{\alpha_1\phi}W^2 \cos\theta \, d\phi \, d\eta$$

and

$$\begin{aligned} V_3 = \int_0^1 \int_0^1 & \frac{(1-\alpha(1-\phi)(1-\eta))(1+\beta_1\phi)^3(1+\beta_2\eta)^3}{\cos^3\theta} \\ & \Big[(W_{\phi\phi})^2 - 4\sin\theta \, W_{\phi\phi}W_{\phi\eta} + 2(1+\sin^2\theta - \nu\cos^2\theta)W_{\phi\phi}W_{\eta\eta} \\ & + 2(1+\nu\cos^2\theta)(W_{\phi\eta})^2 - 4\sin\theta \, W_{\eta\eta}W_{\phi\eta} + (W_{\eta\eta})^2\Big] d\phi \, d\eta \end{aligned}$$

Also

$$\lambda^2 = \frac{12\rho_0\omega^2 a^4(1-\nu^2)}{E_0 h_0^2}$$

is frequency parameter.

Equation (18) involves two unspecified constants i.e. A_1 and A_2 that arise from the substitution of W(x, y). These constants need to be determined as follows:

$$\frac{\partial}{\partial A_i}\left(V_3 - \lambda^2 T_3\right) = 0, \qquad i = 1, 2 \tag{19}$$

On simplifying equation (19) one results,

$$B_{i1}A_1 + B_{i2}A_2 = 0, \qquad i = 1, 2 \tag{20}$$

To obtain a non-trivial solution, the determinant of the coefficient matrix in equation (20) must be zero. Therefore, authors obtain:

$$\begin{vmatrix} B_{11} & B_{12} \\ B_{21} & B_{22} \end{vmatrix} = 0 \tag{21}$$

On solving, equation (21) represents the quadratic equation in λ^{2} out of which two values of lambda (λ_1 & λ_2) can be obtained. These two values will represent first and second mode of frequency simultaneously.

Results And Discussion

α	α_1	β_1 = β_2 = 0.0		β_1 = β_2 = 0.2		β_1 = β_2 =0.4		β_1 = β_2 =0.6		β_1 = β_2 =0.8	
		λ_1	λ_2	λ_1	λ_2	λ_1	λ_2	λ_1	λ_2	λ_1	λ_2
0.0	0.05	192.48	49.96	234.10	60.80	282.07	73.35	336.37	87.57	397.0	103.44
	0.10	190.07	49.34	231.13	60.04	278.43	72.42	331.98	86.46	391.72	102.12
	0.15	187.68	48.72	228.17	59.28	274.83	71.50	327.64	85.35	386.59	100.81
	0.20	185.31	48.11	225.25	58.53	271.25	70.59	323.33	84.26	381.45	99.51
0.2	0.05	187.81	48.74	229.18	59.52	276.84	71.99	330.78	86.11	391.01	101.86
	0.10	185.46	48.13	226.27	58.78	273.27	71.08	326.47	85.02	385.86	100.56
	0.15	183.13	47.53	223.38	58.04	269.73	70.18	322.19	83.93	380.75	99.27
	0.20	180.82	46.93	220.51	57.30	266.23	69.29	317.96	82.86	375.7	97.99
0.4	0.05	183.03	47.48	224.15	58.22	271.51	70.61	325.11	84.62	384.93	100.24
	0.10	180.74	46.89	221.30	57.49	268.01	69.72	320.87	83.55	379.86	98.96
	0.15	178.47	46.31	218.48	56.76	264.54	68.83	316.66	82.48	374.83	97.69
	0.20	176.21	45.73	215.67	56.05	261.10	67.96	312.50	81.43	369.85	96.44
0.6	0.05	178.11	46.20	219.01	56.88	266.08	69.19	319.33	83.10	378.76	98.59
	0.10	175.89	45.62	216.22	56.17	262.65	68.32	315.16	82.05	373.77	97.33
	0.15	173.68	45.05	213.46	55.46	259.25	67.45	311.03	81.00	368.82	96.08
	0.20	171.48	44.49	210.72	54.76	255.88	66.59	306.94	79.97	363.92	94.85
0.8	0.05	173.06	44.87	213.74	55.51	260.53	67.74	313.44	81.54	372.48	96.89
	0.10	170.90	44.31	211.02	54.81	257.17	66.89	309.36	80.51	367.57	95.66
	0.15	168.75	43.76	208.33	54.12	253.84	66.04	305.30	79.48	362.71	94.43
	0.20	166.62	43.21	205.65	53.44	250.54	65.20	301.28	78.47	357.89	93.22

TABLE 1: Frequency vs structural parameters for C-C-C-C at θ = 30°

α	α_1	β_1 = β_2 = 0.0		β_1 = β_2 = 0.2		β_1 = β_2 =0.4		β_1 = β_2 =0.6		β_1 = β_2 =0.8	
		λ_1	λ_2	λ_1	λ_2	λ_1	λ_2	λ_1	λ_2	λ_1	λ_2
0.0	0.05	298.30	78.38	362.57	95.37	436.19	114.96	519.18	137.13	611.53	161.84
	0.10	294.57	77.41	357.96	94.17	430.57	113.51	512.41	135.39	603.48	159.77
	0.15	290.86	76.44	353.38	92.98	425.00	112.07	505.70	133.66	595.51	157.72
	0.20	287.19	75.48	348.85	91.81	419.47	110.64	499.05	131.95	587.60	155.7
0.2	0.05	291.17	76.49	354.97	93.38	428.05	112.85	510.42	134.85	602.08	159.36
	0.10	287.53	75.54	350.46	92.21	422.53	111.42	503.76	133.14	594.16	157.32
	0.15	283.91	74.59	345.98	91.04	417.06	110.01	497.17	131.44	586.30	155.31
	0.20	280.33	73.66	341.54	89.89	411.64	108.61	490.63	129.76	578.52	153.31
0.4	0.05	283.86	74.54	347.21	91.34	419.75	110.69	501.51	132.53	592.49	156.83
	0.10	280.31	73.62	342.79	90.20	414.34	109.28	494.97	130.84	584.68	154.82
	0.15	276.79	72.70	338.42	89.06	408.98	107.90	488.49	129.17	576.95	152.84
	0.20	273.29	71.79	334.07	87.94	403.66	106.53	482.06	127.52	569.29	150.88
0.6	0.05	276.36	72.55	339.27	89.26	411.29	108.48	492.44	130.15	582.73	154.24
	0.10	272.90	71.64	334.96	88.14	405.99	107.10	486.02	128.49	575.06	152.27
	0.15	269.47	70.75	330.68	87.03	400.73	105.74	479.65	126.85	567.45	150.32
	0.20	266.07	69.86	326.44	85.93	395.52	104.40	473.34	125.23	559.92	148.39
0.8	0.05	268.65	70.50	331.14	87.13	402.65	106.21	483.20	127.71	572.82	151.59
	0.10	265.29	69.62	326.93	86.03	397.46	104.87	476.90	126.08	565.28	149.65
	0.15	261.96	68.75	322.76	84.95	392.31	103.54	470.65	124.48	557.80	147.73
	0.20	258.65	67.89	318.62	83.88	387.21	102.22	464.46	122.89	550.39	145.84

TABLE 2: Frequency vs structural parameters for C-C-C-C at θ = 45°

α	α_1	β_1 = β_2 = 0.0		β_1 = β_2 = 0.2		β_1 = β_2 =0.4		β_1 = β_2 =0.6		β_1 = β_2 =0.8	
		λ_1	λ_2	λ_1	λ_2	λ_1	λ_2	λ_1	λ_2	λ_1	λ_2
0.0	0.05	190.02	29.14	232.34	35.65	283.33	43.51	342.91	52.67	410.97	63.10
	0.10	187.64	28.77	229.36	35.20	279.63	42.95	338.36	51.99	405.44	62.28
	0.15	185.27	28.41	226.40	34.75	275.95	42.40	333.84	51.32	399.96	61.47
	0.20	182.92	28.06	223.46	34.31	272.31	41.86	329.36	50.66	394.52	60.67
0.2	0.05	185.12	28.32	227.65	34.84	278.8	42.68	338.44	51.80	406.50	62.17
	0.10	182.79	27.97	224.73	34.40	275.15	42.14	333.95	51.14	401.03	61.37
	0.15	180.49	27.62	221.83	33.96	271.54	41.60	329.49	50.48	395.61	60.57
	0.20	178.20	27.27	218.95	33.53	267.94	41.06	325.07	49.83	390.22	59.79
0.4	0.05	180.08	27.48	222.87	34.01	274.18	41.84	333.91	50.92	401.98	61.23
	0.10	177.82	27.13	220.02	33.58	270.60	41.30	329.48	50.27	396.57	60.44
	0.15	175.57	26.79	217.18	33.15	267.04	40.78	325.08	49.62	391.21	59.66
	0.20	173.34	26.46	214.36	32.73	263.51	40.25	320.72	48.98	385.88	58.88
0.6	0.05	174.89	26.61	217.99	33.16	269.49	40.98	329.32	50.02	397.41	60.28
	0.10	172.70	26.28	215.19	32.74	265.97	40.45	324.95	49.38	392.06	59.50
	0.15	170.52	25.95	212.42	32.32	262.47	39.94	320.61	48.75	386.76	58.72
	0.20	168.35	25.62	209.66	31.91	259.00	39.42	316.30	48.11	381.5	57.96
0.8	0.05	169.55	25.71	212.99	32.29	264.72	40.10	324.66	49.11	392.78	59.30
	0.10	167.42	25.39	210.26	31.88	261.26	39.59	320.35	48.48	387.50	58.53
	0.15	165.31	25.07	207.55	31.47	257.82	39.08	316.08	47.85	382.26	57.77
	0.20	163.21	24.75	204.85	31.07	254.41	38.58	311.83	47.23	377.06	57.02

TABLE 3: Frequency vs structural parameters for SS-SS-SS-SS at θ = 30°

α	α_1	β_1 = β_2 = 0.0		β_1 = β_2 = 0.2		β_1 = β_2 =0.4		β_1 = β_2 =0.6		β_1 = β_2 =0.8	
		λ_1	λ_2	λ_1	λ_2	λ_1	λ_2	λ_1	λ_2	λ_1	λ_2
0.0	0.05	291.89	47.80	356.97	58.55	435.56	71.62	527.51	86.92	632.68	104.35
	0.10	288.23	47.21	352.39	57.81	429.87	70.71	520.51	85.80	624.17	103.00
	0.15	284.59	46.61	347.84	57.07	424.22	69.80	513.56	84.69	615.72	101.67
	0.20	280.98	46.03	343.33	56.35	418.61	68.91	506.67	83.60	607.35	100.34
0.2	0.05	284.30	46.44	349.74	57.22	428.56	70.28	520.62	85.53	625.78	102.87
	0.10	280.74	45.86	345.26	56.50	422.96	69.39	513.71	84.43	617.36	101.54
	0.15	277.20	45.28	340.80	55.78	417.40	68.50	506.85	83.34	609.01	100.22
	0.20	273.68	44.71	336.38	55.07	411.88	67.62	500.04	82.26	600.72	98.92
0.4	0.05	276.51	45.03	342.36	55.86	421.44	68.92	513.63	84.11	618.81	101.37
	0.10	273.04	44.47	337.97	55.15	415.93	68.04	506.81	83.03	610.48	100.05
	0.15	269.60	43.91	333.61	54.45	410.47	67.17	500.04	81.96	602.22	98.76
	0.20	266.17	43.36	329.28	53.76	405.04	66.31	493.33	80.90	594.03	97.47
0.6	0.05	268.49	43.58	334.82	54.46	414.20	67.52	506.54	82.67	611.75	99.83
	0.10	265.12	43.03	330.52	53.77	408.79	66.66	499.82	81.61	603.52	98.54
	0.15	261.78	42.49	326.26	53.09	403.41	65.81	493.14	80.55	595.36	97.26
	0.20	258.45	41.96	322.02	52.42	398.08	64.97	486.52	79.51	587.25	96.00
0.8	0.05	260.22	42.07	327.10	53.03	406.83	66.10	499.36	81.19	604.62	98.27
	0.10	256.96	41.54	322.90	52.36	401.52	65.26	492.73	80.15	596.48	97.00
	0.15	253.72	41.02	318.74	51.70	396.24	64.42	486.15	79.12	588.41	95.74
	0.20	250.50	40.51	314.60	51.04	391.00	63.60	479.62	78.10	580.40	94.49

TABLE 4: Frequency vs structural parameters for SS-SS-SS-SS at θ = 45°

Numerical frequencies for the first two modes of vibration are calculated for h_0 = 0.01M and ν = 0.345. Since the numeric values of both the modes of frequencies obtained in this study for various structural parameters (α, α_1, and β_1 = β_2) and different boundary conditions, the authors have tried to summarize the numerical results in a tabular form as follows:

The results presented in Table *1* demonstrate the variation of the first two natural frequencies (λ_1 and λ_2) with respect to the parameters α, α_1, and $\beta_1 = \beta_2$ at a skew angle of θ = 30° under clamped boundary conditions. It is observed that both λ_1 and λ_2 increase monotonically with increasing taper parameter $\beta_1 = \beta_2$.

For instance, at α = 0.0 and $\alpha_1 = 0.05$, λ_1 increases from 49.96 to 103.44, while λ_2 increases from 192.48 to 397.0 as $\beta_1 = \beta_2$ varies from 0.0 to 0.8. This behavior indicates that the taper parameter induces a stiffening effect on the plate, resulting in higher natural frequencies. A similar trend is observed for higher values of α. However, for fixed α_1, an increase in α leads to a reduction in both λ_1 and λ_2. For example, at $\beta_1 = \beta_2 = 0.0$, λ_1 decreases from 49.96 to 44.87 and λ_2 decreases from 192.48 to 173.06 as α increases from 0.0 to 0.8 because the increasing α reduces the effective young's modulus and consequently the flexural rigidity of the plate, leading to lower stiffness and hence, lower vibration frequency. Furthermore, for fixed α and $\beta_1 = \beta_2$, both frequencies decrease gradually with increasing α_1, highlighting the effect of material non-homogeneity on the dynamic response of the plate. The physical interpretation of the decay in frequency with increasing α_1 is directly associated with the reduction in effective rigidity of the plate. As the non-homogeneity constant increases, the elastic properties of the material vary more significantly throughout the plate domain, which weakens the restoring force developed during vibration. Consequently, the structure becomes more flexible, leading to lower frequencies.

Table *2* presents the corresponding results at θ = 45° for clamped boundary conditions. The observed trends remain consistent with those at θ = 30°, although the magnitude of both frequencies is higher, indicating an increase in structural stiffness with skew angle.

For simply supported boundary conditions, the frequency variations at θ = 30° and θ = 45° are summarized in Tables *3* and 4, respectively. While the qualitative trends remain unchanged, the frequencies are comparatively lower than those for clamped boundary conditions. In particular, the second mode frequency is significantly reduced in the simply supported case as $\beta_1 = \beta_2$ increases, reflecting the reduced constraint at the boundaries.

Comparison

To validate the present formulation, the obtained frequencies have been compared with results available in previously published studies [6] (homogeneous plate). The comparison results at corresponding values of parameters are summarized in Table *5*. It is clearly seen that when the non-homogeneity parameter is taken as 0.5 in the present study, the frequencies (both the modes) are found to be higher than [6] at α = 0.4. However, when the thermal gradient increases from 0.0 to 0.8, the influence of temperature becomes more dominant, and both the modes of frequency become lower than [6]. It proves that even minor changes in material distribution or temperature play a vital role in obtaining the frequencies and hence cannot be neglected.

[6]	Mode 1	Mode 2	Present Study	Mode 1	Mode 2
alpha = 0.4, alpha_1 = 0.0	45.24	174.29	alpha = 0.4, alpha_1 = 0.05	47.48	183.03
alpha = 0.8, alpha_1 = 0.0	49.75	191.5	alpha = 0.8, alpha_1 = 0.05	44.87	173.06

TABLE 5: Comparison of present study with [6] at $\beta_1 = \beta_2 = 0.0$

Conclusions

The primary objective of this study is to investigate the impact of the plate's parameters on the frequencies of thermally induced vibration of a tapered rhombic plate. With the help of findings of this study, we may conclude the present investigation as follows:

Impact of $\beta_1 = \beta_2$ on frequency

At fixed values of thermal gradient and non-homogeneity constant, both the modes of frequency rise significantly as $\beta_1 = \beta_2$ moves from 0.0 to 0.8. This sharp rise suggests that $\beta_1 = \beta_2$ exerts a dominant influence on the vibrational response of the plate.

Influence of α on frequency

Comparing different values of α reveals that increasing α tends to reduce the baseline values of λ_1 and λ_2, though the rate of increase with $\beta_1 = \beta_2$ remains substantial. This reduction in baseline suggests that α has a moderating effect on λ_1 and λ_2, potentially dampening their initial values before the influence of $\beta_1 = \beta_2$ becomes significant.

Comparison across α_1 values

When examining different α_1 values, the results show that higher α_1 generally corresponds to lower values of both λ_1 and λ_2. This trend suggests that increasing α_1 has a similar moderating effect on both the modes.

Effect of skewness on frequency

As skewness of the rhombic plate increases from 30° to 45°, frequency rapidly increases for both modes of vibration. It shows that skewness may become an integral part of the system's dynamic behavior.

Key observations

(i) λ_1 and λ_2 consistently increase with rising $\beta_1 = \beta_2$, regardless of the values of α and α_1. The relationship appears to be linear, suggesting a direct proportionality between $\beta_1 = \beta_2$ and these variables.

(ii) Higher α and α_1 reduce the baseline values of λ_1 and λ_2, but the overall increase with $\beta_1 = \beta_2$ remains robust.

(iii) The data suggest that the combined influence of α, α_1, and $\beta_1 = \beta_2$ governs the system's response, with $\beta_1 = \beta_2$ being the dominant factor driving changes in λ_1 and λ_2.

The authors concluded that by appropriate tapering and by choosing suitable values of structural parameters, we can obtain the desired values of frequency, thus improving the performance of the structure.

For the C-C-C-C and SS-SS-SS-SS boundary conditions, the authors analyzed the plate's sensitivity to changes in the parameter $\beta 1 = \beta 2$ through a frequency gain factor (FGF), which is defined as the relative change in both the modes of natural frequency with respect to a chosen reference configuration. Here authors chose $\beta 1 = \beta 2 = 0.0$ as reference value as given in the following formula:

$$\mathrm{FGF} = \frac{\mathrm{Frequency}(\beta_1 = \beta_2 = 0.8) - \mathrm{Frequency}(\beta_1 = \beta_2 = 0.0)}{\mathrm{Frequency}(\beta_1 = \beta_2 = 0.0)}$$

FGF quantifies the relative increase in frequencies from β_1 = β_2 = 0.0 to β_1 = β_2 = 0.8. This analysis reveals that, when frequencies of the rhombic plate under both boundary conditions vary as β_1 = β_2 grow, the SS-SS-SS-SS configuration consistently shows a higher FGF for both modes of vibration across various values of α and α_1. This indicates that the plate with a simply supported boundary condition is more responsive to changes in system stiffness, effectively acting as a more adaptable system while plates with clamped boundary conditions favor reliability and structural rigidity. The study demonstrates that by appropriate selection of geometric and material parameters, the vibrational characteristics of the plate can be effectively tuned. These findings are particularly useful in the design of engineering structures subjected to thermal environments, where precise control of dynamic behavior is essential.

Additional Information

Author Contributions

All authors have reviewed the final version to be published and agreed to be accountable for all aspects of the work.

Concept and design: Narinder Kaur, Samta Jain, Anupam Khanna

Acquisition, analysis, or interpretation of data: Narinder Kaur, Samta Jain, Anupam Khanna

Drafting of the manuscript: Narinder Kaur, Samta Jain

Critical review of the manuscript for important intellectual content: Narinder Kaur, Anupam Khanna

Supervision: Narinder Kaur, Anupam Khanna

Disclosures

Human subjects: All authors have confirmed that this study did not involve human participants or tissue. **Animal subjects:** All authors have confirmed that this study did not involve animal subjects or tissue. **Conflicts of interest:** In compliance with the ICMJE uniform disclosure form, all authors declare the following: **Payment/services info:** All authors have declared that no financial support was received from any organization for the submitted work. **Financial relationships:** All authors have declared that they have no financial relationships at present or within the previous three years with any organizations that might have an interest in the submitted work. **Other relationships:** All authors have declared that there are no other relationships or activities that could appear to have influenced the submitted work.

Data Availability Statements

The datasets (and/or code) supporting this study are available from the corresponding author upon reasonable request.

References

1. Chakraverty S: Vibration of Plates. CRC Press, Boca Raton; 2008. 10.1201/9781420053968
2. Chakraverty S, Pradhan KK: Free vibration of functionally graded thin rectangular plates resting on Winkler elastic foundation with general boundary conditions using Rayleigh-Ritz method. International Journal of Applied Mechanics. 2014, 6:1450043. 10.1142/s1758825114500434

3. Gorman DJ: Accurate free vibration analysis of rhombic plates with simply-supported and fully-clamped edge conditions. Journal of Sound and Vibration. 1988, 125:281-290. 10.1016/0022-460x(88)90283-0

4. Leissa AW, Laura PAA, Gutierrez RH: Vibrations of rectangular plates with non-uniform elastic edge supports. Journal of Applied Mechanics. 2010, 47:891-895.

5. Azam MS, Ranjan V, Kumar B: Free vibration analysis of rhombic plate with central crack. The International Journal of Acoustics and Vibration. 2017, 22:481-492. 10.20855/ijav.2017.22.4494

6. Gupta AK, Kumar M, Kumar S, Khanna A: Thermal effect on vibration of parallelogram plate of bi-direction linearly varying thickness. Applied Mathematics. 2011, 2:33-38. 10.4236/am.2011.21004

7. Ansari MI, Kumar A, Barnat-Hunek D, Brzyski P: Dynamic analysis of FGM rhombic plates with a variation in the mass. Materials and Technologies. 2018, 6:731-736.

8. Huang CS, McGee OG, Leissa AW, Kim JW: Accurate vibration analysis of simply supported rhombic plates by considering stress singularities. Journal of Vibration and Acoustics. 1995, 117:245-251. 10.1115/1.2874440

9. Kaur N, Khanna A, Ozer O: Thermoelastic vibrational analysis of tapered triangular plates with different boundary conditions. Mechanics of Solids. 2023, 58:1370-1377. 10.3103/s002565442360085x

10. Khanna A, Kaur N: Effect of non-linear thickness variation on vibration of visco-elastic clamped rectangular plate under thermal condition. International Journal of Acoustics and Vibration. 2023, 23:441-447.

11. Khanna A, Sharma AK: Vibration characterization of C-C-C-C visco-elastic square plate with varying temperature. International Journal of Research in Engineering and Applied Sciences. 2012, 2:1754-1760.

12. Khanna A, Sharma N, Kaur N: Free vibrations of non-homogeneous tapered square plate with bi-directional temperature variations. International Journal of Applied Research in Mechanical Engineering. 2012, 2:28-31.

13. Kumar SS, Kumar SA: A computational model on vibration of square plate with varying thickness and thermal effect in two directions. Research Journal of Engineering Sciences. 2013, 2:6-9.

14. Leissa AW: Vibrations of plates. NASA SP-160. NASA, Washington, DC; 1969.

15. Li W: Vibration analysis of rectangular plate with general elastic boundary supports. Journal of Sound and Vibration. 2004, 273:619-635.

16. Malhotra SK, Ganesa N, Veluswami MA: Effect of fibre orientation and boundary conditions on the vibration behaviour of orthotropic rhombic plates. Composites. 1988, 19:127-132.

17. Singha MK, Ramachandra LS, Bandyopadhyay JN: Vibration behavior of thermally stressed composite skew plate. Journal of Sound and Vibration. 2006, 296:1093-1102. 10.1016/j.jsv.2006.01.070

18. Wang X, Wu Z: Differential quadrature analysis of free vibration of rhombic plates with free edges. Applied Mathematics and Computation. 2013, 225:171-183. 10.1016/j.amc.2013.09.018